REPORT DOCUMENTATION PAGE

Form Approved OMB NO. 0704-0188

1. REPORT DATE (DD-MM-YYYY)	2. REPORT TYPE	3. DATES COVERED (From - To)
17-08-2009	Final Report	15-Sep-2008 - 14-Jun-2009

4. TITLE AND SUBTITLE	5a. CONTRACT NUMBER
A tunable magnetic trap platform for single particle manipulation	W911NF-08-1-0455
	5b. GRANT NUMBER
	5c. PROGRAM ELEMENT NUMBER
	611102

6. AUTHORS	5d. PROJECT NUMBER
R. Sooryakumar	5e. TASK NUMBER
	5f. WORK UNIT NUMBER

7. PERFORMING ORGANIZATION NAMES AND ADDRESSES	8. PERFORMING ORGANIZATION REPORT NUMBER
Ohio State University Research Foundation Office of Sponsored Programs Ohio State University Research Foundation Columbus, OH 43210 -1063	

9. SPONSORING/MONITORING AGENCY NAME(S) AND ADDRESS(ES)	10. SPONSOR/MONITOR'S ACRONYM(S) ARO
U.S. Army Research Office P.O. Box 12211 Research Triangle Park, NC 27709-2211	11. SPONSOR/MONITOR'S REPORT NUMBER(S) 54199-MS-II.1

12. DISTRIBUTION AVAILIBILITY STATEMENT

Approved for public release; distribution unlimited

13. SUPPLEMENTARY NOTES

The views, opinions and/or findings contained in this report are those of the author(s) and should not contrued as an official Department of the Army position, policy or decision, unless so designated by other documentation.

14. ABSTRACT

In this Short Term Innovative Research (STIR) project, the physics of magnetic traps originating from domain walls in ferromagnetic zigzag wires was investigated. The design and architecture of the network of traps provided the framework for organizing well-defined planar assemblies of micro-particles and tethered biomolecules. A special feature of this platform is the ability to continuously tune the strength of the trapping potential through external magnetic fields that also render the traps to be mobile.

15. SUBJECT TERMS

Magnetic Traps, Domain Walls, Micro-manipulation, Micro-particles, Biological Cells

16. SECURITY CLASSIFICATION OF:			17. LIMITATION OF ABSTRACT	15. NUMBER OF PAGES	19a. NAME OF RESPONSIBLE PERSON
a. REPORT	b. ABSTRACT	c. THIS PAGE	SAR		Ratnasingham Sooryakumar
U	U	U			19b. TELEPHONE NUMBER 614-292-3130

Standard Form 298 (Rev 8/98)
Prescribed by ANSI Std. Z39.18

REPORT DOCUMENTATION PAGE (SF298)
(Continuation Sheet)

The **Short Term Innovative Research (STIR)** project began September 15, 2008 and was completed on June 14, 2009. The budget for this 9-month grant was $50 K.

In brief, the project rested on creation of nanoscale magnetic domain walls imprinted on a silicon wafer to produce localized magnetic field gradients that trap *single magnetic microspheres* and *individual biological cells*. We take advantage of highly localized, permanent magnetic field gradients at the vertices of ferromagnetic zigzag wires created on a surface (Fig. 1a) to assemble labeled cells or microspheres onto designed arrays. By combining this platform with externally controlled weak (~60 Oe) fields, programmable directed forces that are gentile enough to not produce damage transport single or multiple cells and inert particles across surfaces.
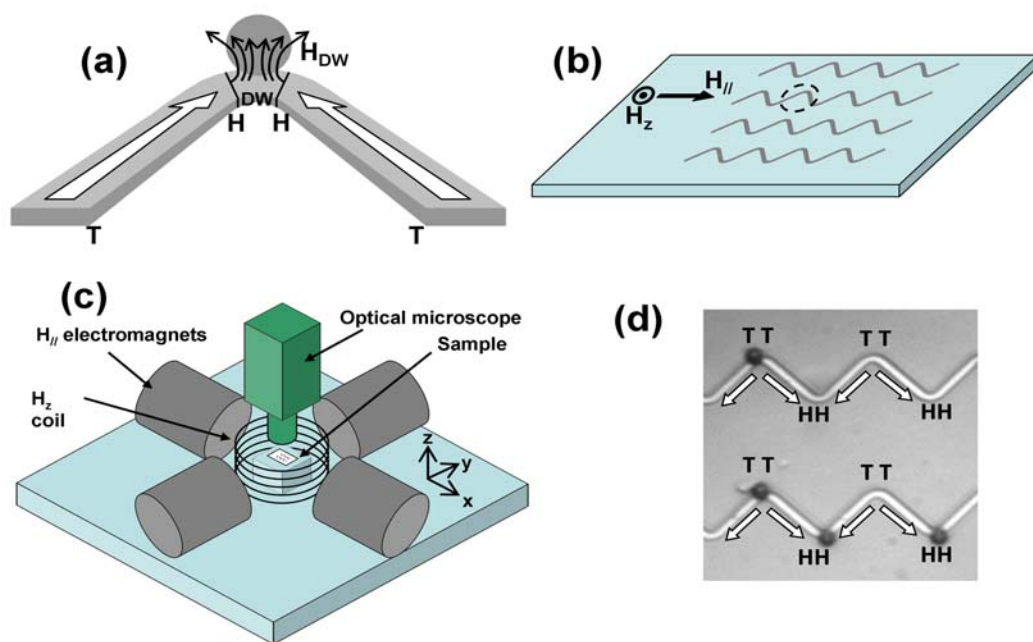

Figure 1: (a) Schematic of rectangular zigzag wire with a head-to-head (HH) domain wall (DW) at the vertex, associated field H_{DW}, and a trapped magnetic particle (gray disk). The HH and tail-to-tail (TT) walls at the turns are created by an one-time momentary 1 kOe in-plane magnetic field. (b) Array of zigzag wires imprinted on platform with perpendicular (H_z) and in-plane ($H_{//}$) magntic fields. Sketch in (a) is enlarged view of the dotted circle around a vertex. (c) Schematic of electromagnets and coil to create $H_{//}$ and H_z. Movement of the microsphere/cell observed by an optical microscope (Reichert) with a 20X objective and high speed camera. (d) Actual image of super-paramagnetic spheres (2.8 µm diameter, dark circles) selectively attracted from solution and trapped only at HH and TT domain walls under no external fields. The FeCo wires imprinted on Si are 2 µm wide, 40 nm thick with 16 µm between adjacent vertices.

Figure 1 illustrates key aspects of the trap platform structure: a set of zigzag $Fe_{0.5}Co_{0.5}$ wires with stationary domain walls (DW) located at wire turns (Fig. 1a, Fig. 1b); the externally applied tuning magnetic fields (Fig. 1c); and microspheres selectively trapped at the domain walls (Fig. 1d). Wires of rectangular cross-section were patterned by

standard electron-beam writing techniques on a Si substrate followed by sputter deposition of a $Fe_{0.5}Co_{0.5}$ film. Head-to-head (HH) and tail-to-tail (TT) domain-walls (Fig. 1a) are created at neighboring vertices by a momentary in-plane external field (~1 kOe). The highly localized trapping fields associated with the wire vertices are evident upon depositing a solution of commonly used magnetic microspheres on the platform. Fig. 1d shows the spheres attracted to and trapped only at the HH and TT domain walls.

Figure 2 show several transporting examples: either microspheres or T-lymphocyte cells, where previously separated T cells (CD3 positive) from human blood cells were labeled with 1 µm anti-CD3 spheres. Figures 2a and 2b show the movement of a microsphere and several T-lymphocyte cells, respectively, above the wire by a sequence of alternating $H_{//}$ and H_z fields with magnitude 60 Oe. Guided by the wire, the remotely directed forces move these objects with an average speed of 20µm/sec from one vertex to the next and beyond by a set of steps as detailed in Fig. 3. The trajectory can be reversed by reordering sequence of the $H_{//}$ and H_z fields. Figure 2c illustrates a sequence of images showing a T-lymphocyte cell transported away from the wires and returned further down the same wire. Depending on the nature of the domain wall (HH or TT), the route and directional forces are regulated by orienting $H_{//}$ (60 Oe) parallel or anti-parallel to the desired planar direction of movement on the platform.
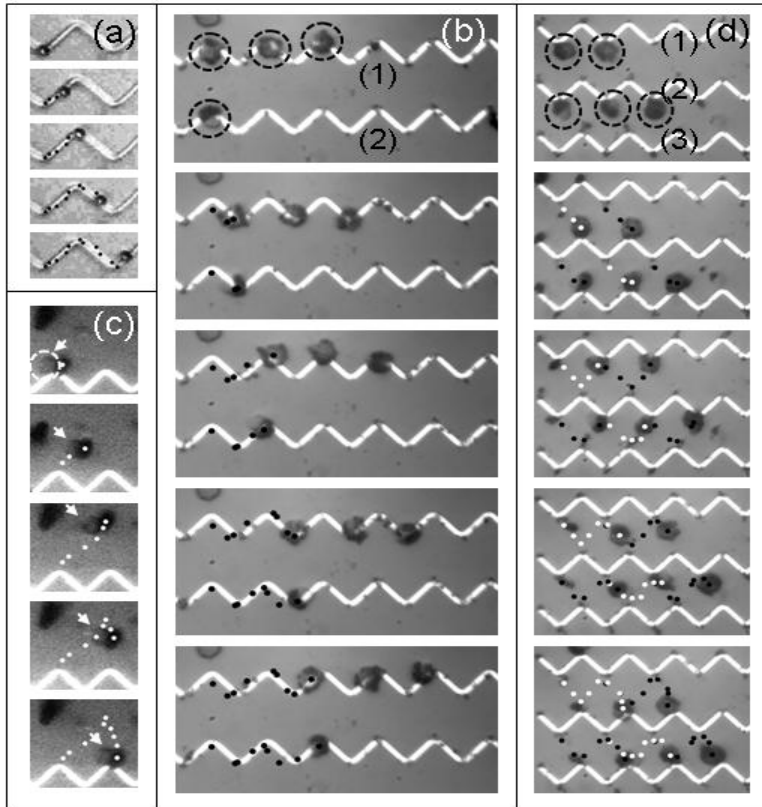

Figure 2. (a) Sequential applications of planar ($H_{//}$) and perpendicular (H_Z) fields transport a microsphere on a Si platform along a zigzag wire. The trajectory of the sphere is indicated by dots. (b) Transport of several T-lymphocyte cells along zigzag wire. The cells (dashed circles in top panel) are conjugated to 1 µm magnetic spheres. (c) Transport of a single T-lymphocyte cell on a trajectory (white dots) away from the wires and its controlled return to neighboring vertex on same wire. The arrows (and dashed circle in first panel) identify the cell. (d) Simultaneous back and forth transport of five fluid borne T-cells between zigzag wire (1) (2) and (3). Dots identify trajectory of four cells.

Figure 2d illustrates the correlated motion of five T-lymphocyte cells from adjacent vertices on one wire to those on the neighboring wire and their return to the first, each shifted one vertex. Reversing the orientation of H_z transforms an attractive HH domain

wall on one wire into a repulsive trap while the cells are transported to an attractive TT trap on the neighboring wire. With in-plane particle trajectories controlled by $H_{//}$, multiple cells or particles are maneuvered in unison between vertices on separated wires while being transported at an average speed of ~ 10 µm/sec.
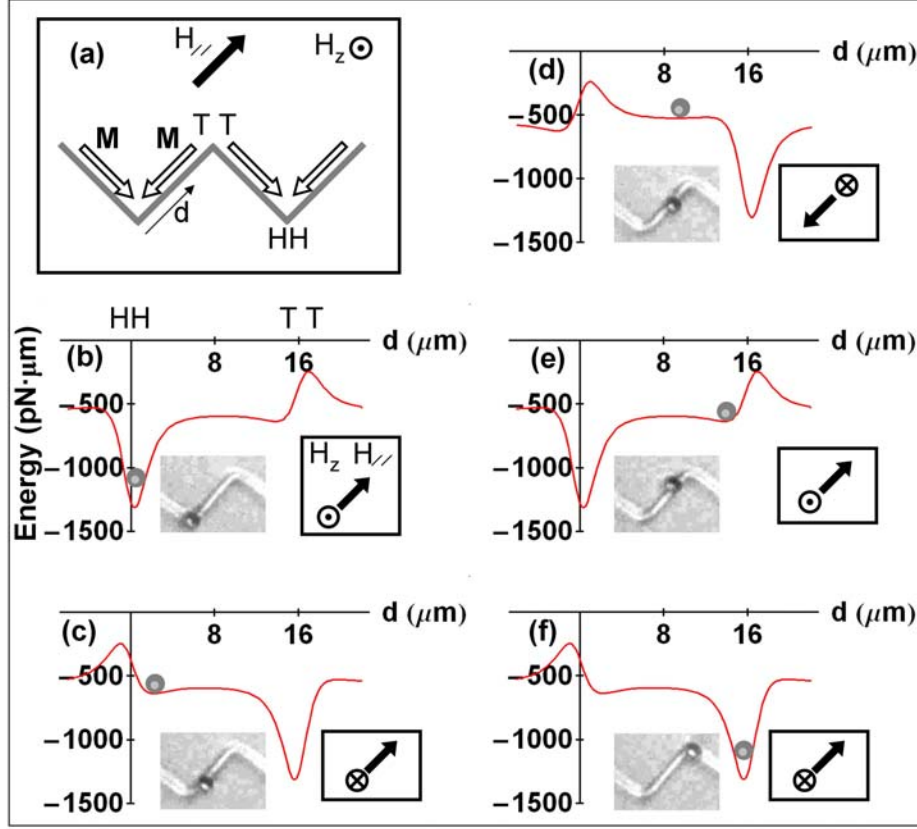

Figure 3. (a) Orientation of zigzag wires, their magnetization M (open arrows), and external $H_{//}$, H_Z fields. (b) – (f) illustrates variation of magnetic potential energy with distance d from the HH vertex along the wire. In each case, orientations of $H_{//}$ and H_z are indicated. Inset photographs show close correlation between locations of microsphere on the wire and the calculated local energy minimum position.

Figure 3 underpins the forward motion illustrated in Figs. 2a, 2b by showing how inverting the energy landscape along the wire assists it. The applicable structure and field geometries are shown in Fig. 3a. Figures 3b – 3f are calculated magnetic energy profiles for a 2.8 µm diameter bead in the presence of H_{DW}, H_z, $H_{//}$. In figure 3b the energy minimum is centered above the head-to-head domain wall vertex. Upon reversing H_z (while $H_{//}$ remains unchanged), the HH trap at the origin transforms to a repulsive site while moving the energy minimum towards the TT trap at the neighboring vertex. The local energy minimum is guided, as shown in Fig. 3d, towards the TT site by reversing $H_{//}$. Upon alternating the sequence of H_z and $H_{//}$ fields, the cell reaches the TT trap at an average speed of 20 µm/sec in our present configuration. Insets in Fig. 3b-3f show actual photographs of the microsphere and their direct correspondence to the energy minimum as it is transported.

Discrete magnetic disks: In this effort we employed reprogrammable magnetization profiles created through lithographically patterned discrete ferromagnetic disks as a template for producing highly localized trapping fields. The resulting tunable magnetic field gradients in the vicinity of the disk periphery enable directed forces to be applied on, (a) immunomagnetically labeled biological cells and, (b) magnetic microspheres that act as magnetically actuated miniature force transmitting probes to navigate fluid borne unlabeled cells with micrometer precision. The principal features of this study are demonstrated by remotely transporting and arranging, with programmed routines (*a la* joystick), multiple or individual T-lymphocyte and leukemia cells. Without producing damage, the gentle forces transport the cells with speeds up to 20 µm/sec across a silicon platform to predetermined sites.

In summary, remotely controlled directed forces from imprinted magnetic wires have enabled the transport of fluid borne individual or multiple T-lymphocyte cells and microspheres at speeds of several microns per second on a silicon platform. Central to these observations are the simple methods to create, with nanoscale precision, highly confined domain wall field gradients. In addition to the convenience of optical microscope observation, development of such mobile magnetic traps will provide real-time analysis of inert microscopic objects and living cells through direct manipulation that offers much more accurate selection than data-averaging over a population of particles and cells.